Active Power Decoupling in Single- and Three-Phase Compatible T-Type AC-DC Converter Using a Built-in Leg

Ryohei Higashide
Dept. of Electrical, Electronics, and Information Engineering
Nagaoka University of Technology
Nagaoka, Japan
s235027@stn.nagaokaut.ac.jp

Hiroki Watanabe
Dept. of Electrical, Electronics, and Information Engineering
Nagaoka University of Technology
Nagaoka, Japan
hwatanabe@vos.nagaokaut.ac.jp

Jun-ichi Itoh
Dept. of Science of Technology Innovation
Nagaoka University of Technology
Nagaoka, Japan
itoh@vos.nagaokaut.ac.jp

Abstract*— *This paper proposes an active power decoupling (APD) method for single-phase grid operation using a single-phase and three-phase compatible T-type AC-DC converter. The proposed system consists of an AC-DC converter and an APD circuit. In single-phase operation, the APD function is achieved by utilizing the extra leg of the converter, eliminating the need for additional circuitry. A split capacitor on the DC side is used for APD, introducing a trade-off between harmonic reduction enabled by a bidirectional switch and the capacitor voltage amplitude. Simulation results show that the output voltage ripple at twice the grid frequency is reduced by 99.0% with the proposed APD. Additionally, as the capacitor voltage utilization factor decreases, the input current harmonic spectrum approaches that of carrier-level shift modulation. Experimental results show that the second harmonic component of the output voltage is reduced by 96.6%, confirming the effectiveness of the APD function. Furthermore, they show that the harmonic characteristics of the input current closely match the simulation results.

Keywords*—*on-board charger, t-type ac-dc converter, single-phase and three-phase compatibility, active power decoupling

I. Introduction

In recent years, on-board chargers (OBCs) have been actively studied for electric vehicles [1]-[3]. When an OBC connects to a single-phase AC grid, the instantaneous power on the AC side pulsates. Electrolytic capacitors are commonly used in the DC bus in order to absorb power fluctuations. However, using electrolytic capacitors limits the lifespan of power converters because of thermal degradation, as described by the Arrhenius law. To solve this problem, active power decoupling (APD) methods have been proposed [4]-[7]. These approaches aim to decrease the size of power converters and extend their lifespan by replacing electrolytic capacitors with smaller film or ceramic capacitors.

In particular, Ref. [6] and [7] have proposed APD methods that support both single-phase and three-phase AC grids. Ref. [6] has presented an APD method based on an interleaved totem-pole power factor correction (PFC) converter, where the extra leg in single-phase operation is used as a half-bridge APD circuit. This approach eliminates the need for additional APD circuitry. However, the neutral point current required for APD is not adequately supplied to the buffer capacitor due to interference between PFC control and neutral point current control, resulting in remaining pulsation in the DC voltage. Ref. [7] introduces another APD method using the LCL filter of a three-phase PWM rectifier, which also avoids additional circuitry. Nevertheless, the power factor and total harmonic distortion (THD) of the grid current significantly deteriorate because the AC side filter capacitor is repurposed for APD.

This paper proposes an APD method for single-phase grid operation using a single-phase and three-phase compatible T-type AC-DC converter. The proposed control strategy allows independent regulation of the neutral point current and grid current. As a result, residual output voltage pulsation and power factor degradation, which are observed in Refs. [6] and [7] are effectively suppressed. Moreover, by employing the bidirectional switch in the T-type AC-DC converter for multi-level modulation, the proposed method enables miniaturization of the AC-side filter. On the other hand, the DC side capacitor voltage fluctuates at the grid frequency for APD, leading to a trade-off between the amplitude of the capacitor voltage and the harmonic reduction achieved through multi-level modulation.

The originality of this paper clarifies this trade-off and quantitatively evaluates the relationship between capacitor voltage amplitude and harmonic reduction. Simulation results demonstrate that the proposed method reduces the second harmonic component of the output voltage by 99.0%. Additionally, the harmonic component of the input current increases with the capacitor voltage utilization factor, exhibiting intermediate behavior between conventional modulation methods. Experimental results confirmed the APD function of the proposed circuit configuration. The proposed APD method reduces the second harmonic component of the output voltage by 96.6% in the experiment. Furthermore, the harmonic characteristics of the input current closely matched the simulation results.

II. Single-phase and Three-phase Compatible T-type AC-DC Converter

A. Circuit Configuration

Fig. 1 shows the circuit configuration of the single-phase and three-phase compatible T-type AC-DC converter. In three-phase grid operation, the grid is connected to terminals T_U, T_V, and T_W, as shown in Fig. 1(a). In single-phase grid operation, the AC grid is connected to terminals T_U and T_V, while terminal T_W is connected to T_N, as shown in Fig. 1(b). Under this configuration, the circuit functions as a three-phase T-type AC-DC converter in three-phase operation and as a T-type AC-DC converter with a half-bridge APD circuit in single-phase operation. Although the proposed circuit topology differs from that in Ref. [4], it similarly realizes APD by utilizing the extra leg during single-phase operation. Therefore, no additional circuitry is required for APD implementation.

B. Active Power Decoupling

Fig. 2 shows the principle of active power decoupling. In the proposed T-type AC-DC converter, DC side capacitors C_1

and C_2 function as energy buffers for the APD function. Assuming the single-phase grid operates at unity power factor, the instantaneous power on the AC side, p_{in}, is expressed as

$$p_{in} = v_{in} i_{in} = V_{in} I_{in} - V_{in} I_{in} \cos(2\omega t) \tag{1}$$

where v_{in} and i_{in} are the input voltage and current, respectively, V_{in} and I_{in} are their RMS values, and ω is the grid angular frequency. In single-phase systems, the output voltage of the AC-DC converter exhibits a ripple at twice the grid frequency. In order to compensate for this power pulsation, the APD method controls the buffer power p_{buf} in the opposite phase, as shown in Fig. 2.

In the T-type converter, the APD method regulates the DC side capacitor voltages, v_{c1} and v_{c2}, as sinusoidal waveforms with opposite phases, centered around half the DC voltage. These voltages are expressed as

$$\begin{cases} v_{c1} = \dfrac{V_{dc}}{2} + V_c \sin(\omega t - \dfrac{\pi}{4}) \\ v_{c2} = \dfrac{V_{dc}}{2} - V_c \sin(\omega t - \dfrac{\pi}{4}) \end{cases} \tag{2}$$

where V_{dc} is the DC voltage, and V_c is the amplitude of the capacitor voltage, which must be less than half of V_{dc}. For the capacitor voltages in order to match (2), each capacitor current is expressed as

$$\begin{cases} i_{c1} = -\omega C_1 V_c \sin(\omega t + \dfrac{\pi}{4}) \\ i_{c2} = \omega C_2 V_c \sin(\omega t + \dfrac{\pi}{4}) \end{cases} \tag{3}$$

where C_1 and C_2 are the capacitance of the DC side capacitor. From (3), the neutral point current i_n, flowing through the leg formed by the capacitors is derived as

$$i_n = 2\omega C V_c \sin(\omega t + \frac{\pi}{4}) \tag{4}$$

Note that the DC-side capacitors in this paper are each designed with the same capacitance. For this reason, each capacitor is expressed as C in (4). The neutral point current i_n to match (3), the T-type AC-DC converter achieves APD functionality without requiring any additional circuitry.

III. Control Strategy

This section describes the control strategies for the T-type AC-DC converter and the half-bridge APD circuit during single-phase grid operation.

A. *T-type AC-DC Converter*

Fig. 3 shows the operating waveforms of the T-type AC-DC converter. Fig. 3(a) shows the waveform when operating between 0 V and the capacitor voltages v_{c1} and v_{c2}, while Fig. 3(b) shows the waveform when operating between V_{dc} and the capacitor voltages v_{c1} and v_{c2}. The T-type AC-DC converter applies either v_{c1} or v_{c2} to the line voltage v_{rec} when the full-bridge-side switches (S_1 to S_4) and the neutral point switches (S_7, S_8) are turned on simultaneously. Since v_{c1} and v_{c2} differ from V_{dc}, the resulting line voltage v_{rec} forms a multi-level waveform. When v_{c1} and v_{c2} fluctuate for APD, a temporary imbalance in the applied voltage to v_{rec} occurs during each switching period. However, the duration for which each capacitor voltage is applied within a switching cycle remains constant. Moreover, since the capacitor voltages are sinusoidal waveforms with equal amplitude and opposite phase, no steady-state voltage error occurs even if the capacitor voltages fluctuate. Therefore, conventional carrier level-shift modulation can be applied to T-type AC-DC converters with APD.

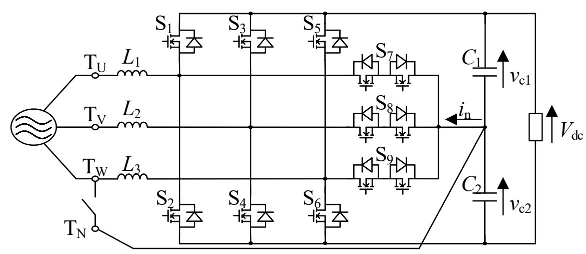

(a) Three-phase grid operation.

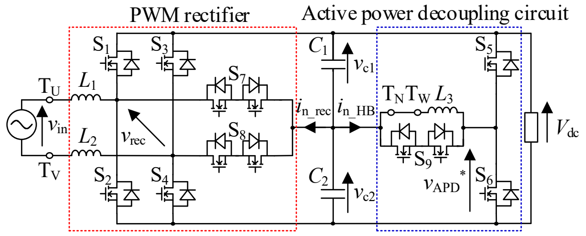

(b) Single-phase grid operation.

Fig. 1. Circuit configuration of the single-phase and three-phase compatible T-type AC-DC converter.

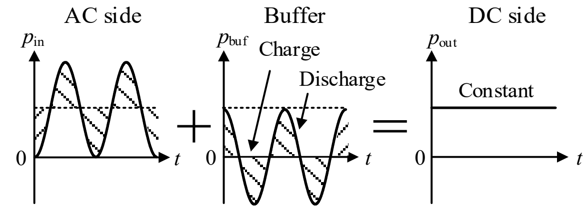

Fig. 2. Principle of active power decoupling function.

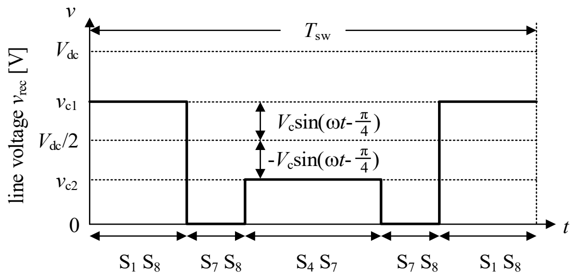

(a) 0 V to v_{c1} v_{c2}.

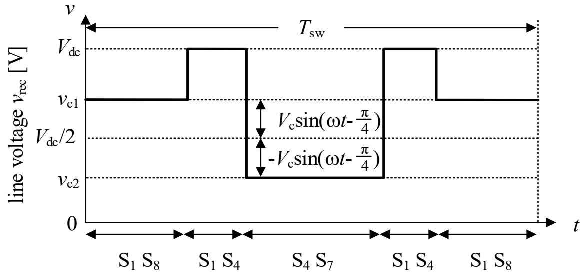

(b) V_{dc} to v_{c1} v_{c2}.

Fig. 3. Operation waveforms of v_{rec}.

Fig. 4 shows the control block diagram of the T-type AC-DC converter. The control block diagram of the T-type AC-DC converter consists of output voltage control and grid current control. The modulation method employed is the conventional carrier level-shift technique.

B. Half-Bridge Active Power Decoupling Circuit

The current from each DC side capacitor splits into two parts: i_{n_rec}, which flows into the T-type AC-DC converter side, and i_{n_HB}, which flows into the half-bridge APD circuit. The i_{n_HB} compensates for both the capacitor voltage fluctuations caused by i_{n_rec} and the power pulsation component at twice the grid frequency.

Fig. 5 shows the control block diagram of the half-bridge APD circuit. This circuit includes two main control functions: capacitor voltage balance control and neutral point current control. The voltage balance control compensates for imbalances caused by i_{n_rec}. Switches S_5 and S_6 operate based on the output voltage command v_{APD}^* from the APD controller. The inductor L_3, through which i_{n_HB} flows, corresponds to the W-phase in three-phase grid operation. Since a current sensor is already installed for this phase, no additional sensor is required for the APD circuit.

IV. SIMULATION RESULTS

Table 1 shows the simulation conditions. The capacitance values of the DC side capacitors C_1 and C_2 are set to 295 µF, resulting in a capacitor voltage utilization factor of 0.8. This factor indicates the ratio of V_c to $V_{dc}/2$.

A. Fundamental operation

Fig. 6 shows simulation results for a T-type AC-DC converter in single-phase grid operation. Fig. 6(a) shows the results without an APD, and Fig. 6(b) shows the results with an APD. As shown in Fig. 6(a), the output voltage pulsates at twice the grid frequency due to power pulsation. Meanwhile, Fig. 6(b) indicates that the DC side capacitor voltages pulsate in the opposite phase, demonstrating the APD function. Consequently, the output voltage remains constant.

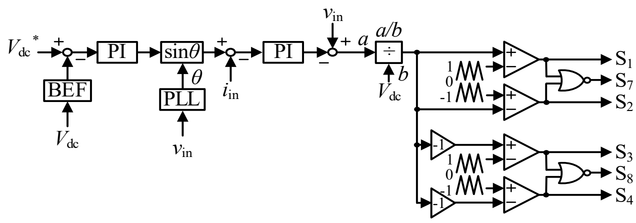

Fig. 4. Control block diagram of T-type AC-DC converter.

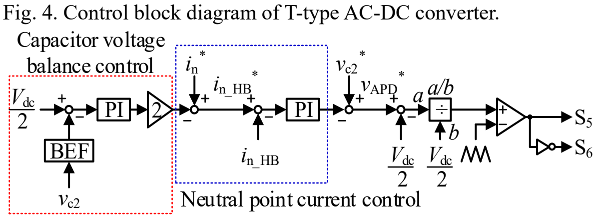

Fig. 5. Control block diagram of half bridge type active power decoupling circuit.

TABLE I. SIMULATION CONDITIONS IN SINGLE-PHASE GRID OPERATION

Parameter		Symbol	Value
Output power		P_{out}	3 kW
Grid voltage		v_{in}	200 V_{rms}
Output voltage		V_{dc}	450 V
Grid frequency		f	50 Hz
Switching frequency		f_{sw}	20 kHz
DC side capacitor		C_1, C_2	295 µF
Capacitor voltage amplitude		V_c	180 V (0.8×V_{dc}/2)
Filter inductor		L_1, L_2, L_3	210 µH (%Z:1.0%)
Response angular frequency	i_{in} control	ω_{in}	3000 rad/s
	i_n control	ω_n	5000 rad/s
	v_{c2} control	ω_{c2}	6.28 rad/s

B. Harmonic Analysis of Output Voltage

Fig. 7 shows the harmonic analysis of the output voltage V_{dc}. The fundamental frequency is 50 Hz, and each harmonic component is normalized to the DC component. With APD applied, the second harmonic component is reduced to 0.2%, representing a 99.0% reduction compared to the case without

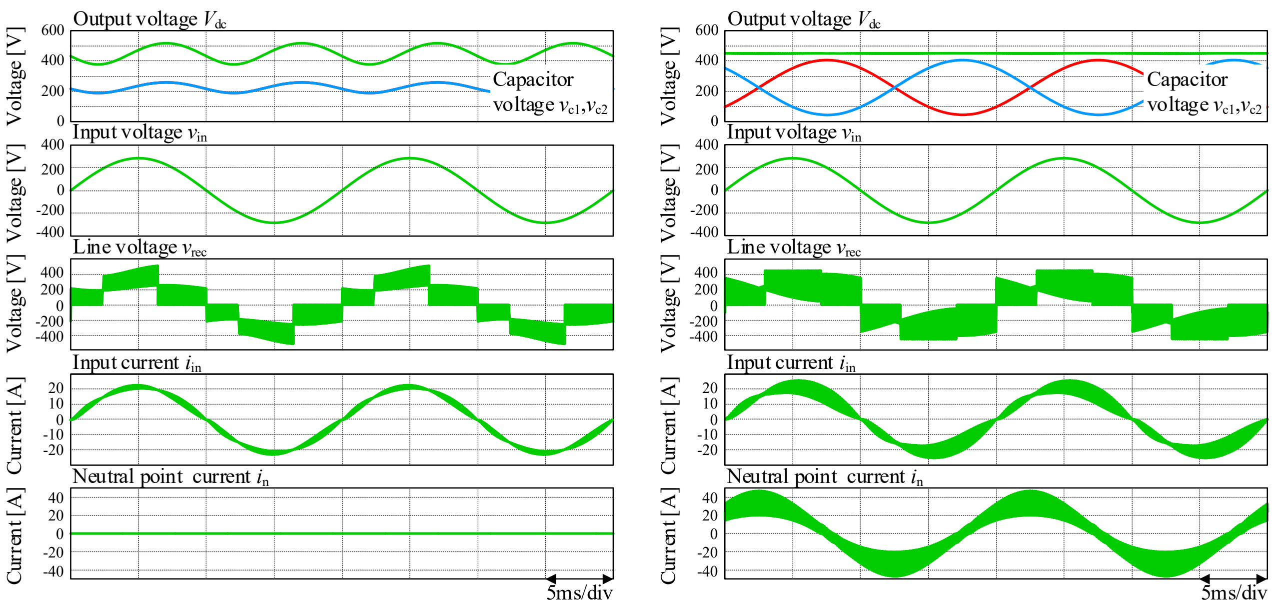

(a) Without active power decoupling

(b) With active power decoupling

Fig. 6. Simulation waveform in a steady state.

APD. This result confirms the effectiveness of the proposed APD method.

C. Harmonic Analysis of Input Current

Fig. 8 shows the harmonic analysis of the input current, corresponding to the results shown in Fig. 6(a) and (b). The vertical axis represents the amplitude of each harmonic normalized by the fundamental amplitude. In Fig. 8(a), the equivalent switching frequency is effectively doubled, similar to a conventional multi-level converter. In contrast, Fig. 8(b) shows that harmonics appear at integer multiples of the switching frequency and its sidebands. This is due to the DC side capacitor voltages v_{c1} and v_{c2} pulsating at the grid frequency. These results indicate a trade-off between the capacitor voltage utilization factor and the harmonic reduction of the input current i_{in}.

Fig. 9 shows the RMS values of the input current harmonics and the corresponding DC side capacitance values as the capacitor voltage utilization factor varies. The horizontal axis represents the capacitor voltage utilization factor, while the secondary vertical axis indicates the required capacitance of the DC side capacitors. Harmonic components are calculated up to 200 kHz. Fig. 9 compares the harmonic performance of carrier level-shift modulation (with and without APD) and unipolar modulation. As shown in Fig. 9, when the capacitor voltage utilization factor is small, the DC side capacitor voltages approximate the balanced state of a conventional multi-level converter, resulting in lower RMS harmonic values. Thus, reducing the capacitor voltage utilization factor can lead to smaller AC side filter sizes. However, the required capacitance is inversely proportional to the square of the capacitor voltage utilization factor, meaning that a lower capacitor voltage utilization factor significantly increases the required capacitance. Consequently, a trade-off exists between minimizing the size of the DC side capacitors and the AC side filter. Harmonic reduction benefits are observed when the capacitor voltage utilization factor ranges from 0.1 to 0.6, compared to unipolar modulation. Therefore, future work will focus on optimizing the volume of both the DC side capacitors and the AC side filter within this range.

V. Experimental Results

In order to verify the effectiveness of the proposed APD method, a 3-kW prototype was developed. The experiment is conducted under the conditions listed in Table 1, using IMW65R026M2H (Infineon) as the switching devices.

A. Fundamental operation

Fig. 10 shows the experimental results of the T-type AC-DC converter in single-phase grid operation. Fig. 10(a) shows the result without APD, while Fig. 10(b) shows the result with APD. In Fig. 10(a), the capacitor voltages pulsate at twice the grid frequency due to power pulsations. This causes the DC voltage to pulsate without an APD. In contrast, as shown in Fig. 10(b), the DC side capacitor voltages are controlled by the APD circuit in order to match (2), thereby suppressing the pulsation of the DC voltage. Consequently, the DC side capacitor voltage pulsation component is superimposed on the line voltage v_{rec}. Additionally, the input current ripple is pulsating.

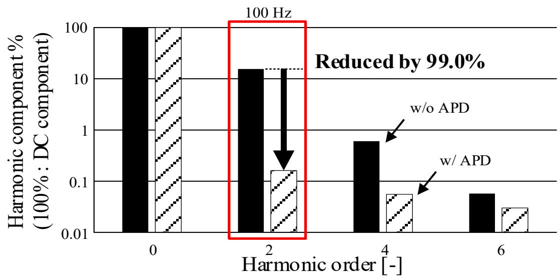

Fig. 7. Harmonic analysis of the output voltage.

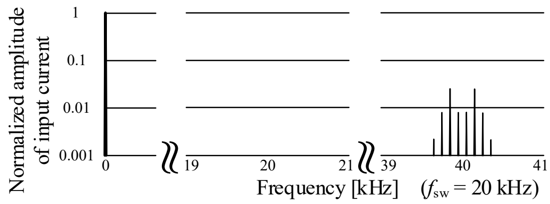

(a) Without APD

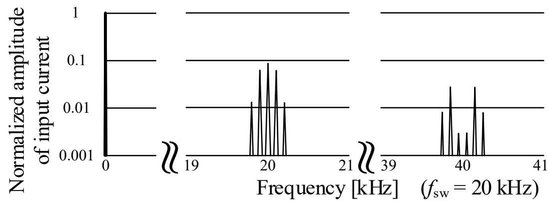

(b) With APD

Fig. 8. Harmonic analysis of the input current in the simulation.

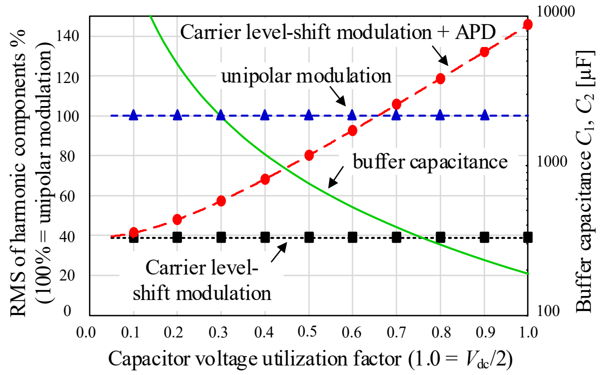

Fig. 9. RMS characteristics of input current harmonics and buffer capacitance. (calculated to 200 kHz)

B. Harmonic Analysis of Output Voltage

Fig. 11 shows the harmonic analysis of the output voltage V_{dc}. The fundamental frequency is 50 Hz, and each harmonic component is normalized to the DC component. With APD applied, the second harmonic component is reduced to 0.5%, representing a 96.6% reduction compared to the case without APD. However, the reduction effect on second-order harmonic components has deteriorated compared to the simulation. The reason for this is the error introduced by assuming a unity power factor when deriving the capacitor voltage and neutral point current. Nevertheless, the results in Fig. 11 indicate sufficient harmonic reduction effectiveness, confirming the validity of the proposed APD method.

C. Harmonic Analysis of Input Current

Fig. 12 shows the harmonic analysis of the input current measured in the experiment. Fig. 12(a) and (b) correspond to the experimental results shown in Fig. 10(a) and (b), respectively. The vertical axis represents the amplitude of each harmonic normalized by the fundamental component. In

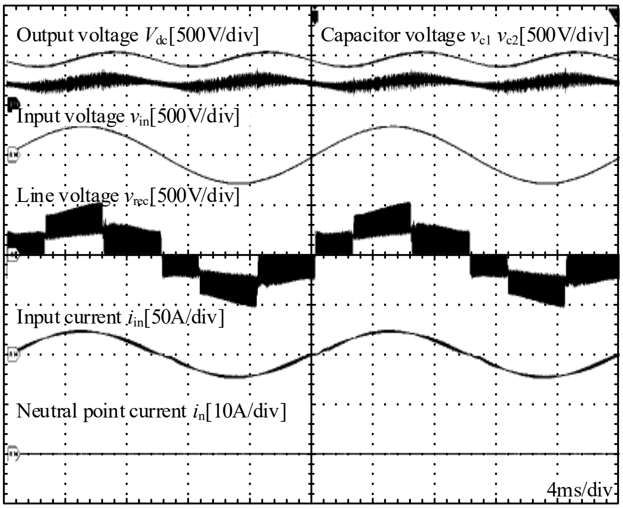

(a) Without active power decoupling

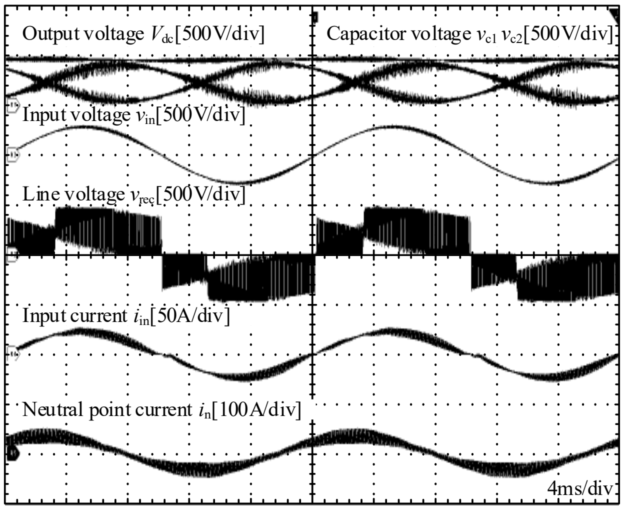

(b) With active power decoupling

Fig. 10. Experimental result in a steady state.

Fig. 12(a), similar to conventional multi-level converters, the dominant harmonic spectrum appears around twice the switching frequency. A minor spectral component near the switching frequency is attributed to common-mode current and power pulsations. In contrast, Fig. 12(b) shows that harmonics at the switching frequency and its sidebands dominate due to the capacitor voltage pulsation of the APD function. This result closely matches the simulation outcome shown in Fig. 8.

VI. Conclusion

This paper proposed an active power decoupling method for single-phase grid operation using a single-phase and three-phase compatible T-type AC-DC converter. The proposed circuit configuration operates as a three-phase T-type AC-DC converter under three-phase grid conditions and as a T-type AC-DC converter with a half-bridge APD circuit under single-phase operation. Simulation results demonstrated that the proposed APD method reduces the second harmonic component of the output voltage by 99.0%. Additionally, the trade-off between miniaturizing the DC side capacitors and the AC side filter is clarified. Experimental results confirmed the APD function of the proposed circuit configuration. The proposed APD method reduces the second harmonic component of the output voltage by 96.6% in the experiment. Furthermore, the harmonic characteristics of the input current closely matched the simulation results.

Future work will focus on optimizing the capacitor voltage utilization factor.

Acknowledgment

This work was supported by JST SPRING, Japan Grant Number JPMJSP2189.

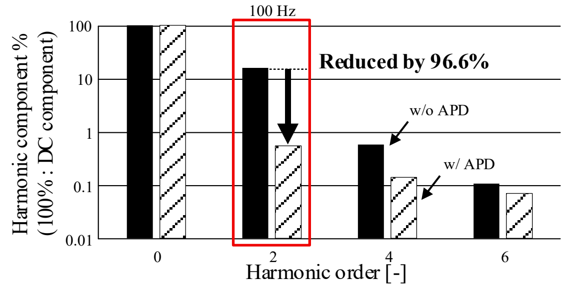

Fig. 11. Harmonic analysis of the output voltage.

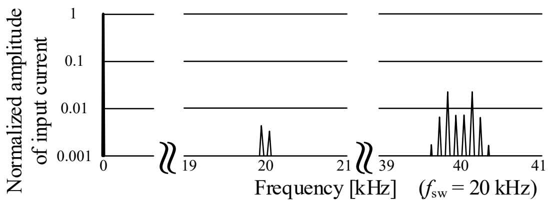

(a) Without active power decoupling

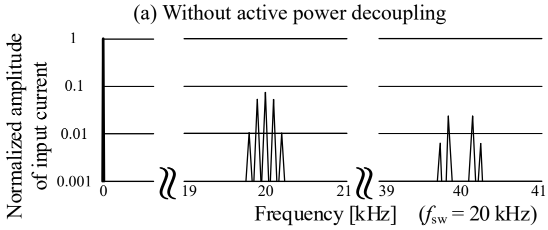

(b) With active power decoupling

Fig. 12. Harmonic analysis of the input current in the experiment.

References

[1] R. Emoto, S. Okamoto, F. Ikeda, M. Okamoto, H. Yamada, and T. Tanaka, "Control Strategy of Discharged Power with Bidirectional Battery Charger for EVs to Prevent Reverse Power Flow to Utility Grid," in IEEJ Journal of Industry Applications, vol. 13, no. 3, pp. 346-347, Feb. 2024

[2] T. Kimura, T. Yamada, R. Kazaoka, and T. Noguchi, "Control Method of Dual Inverter System for EV with One Battery," in IEEJ Journal of Industry Applications, vol. 12, no. 3, pp. 376-383, Dec. 2023

[3] S. G. Barbosa, L. H. S. C. Barreto and D. d. S. Oliveira, "A Single-Stage Bidirectional AC–DC Converter Feasible for Onboard Battery Chargers," in IEEE Journal of Emerging and Selected Topics in Power Electronics, vol. 10, no. 3, pp. 3024-3032, Jun. 2022

[4] Shohei Komeda, Shunsuke Takuma, Yoshiya Ohnuma, Ryo Gondo, Daisuke Maezaki, and Noritaka Taguchi, "Operation Characteristics of Discontinuous Current Mode for a Dual-Active-Bridge AC-DC Converter with an Active Energy Buffer," in IEEJ Journal of Industry Applications, vol. 12, no. 5, pp. 1015-1024, Jun. 2023

[5] H. V. Nguyen, D. -D. To and D. -C. Lee, "Onboard Battery Chargers for Plug-in Electric Vehicles With Dual Functional Circuit for Low-Voltage Battery Charging and Active Power Decoupling," in IEEE Access, vol. 6, pp. 70212-70222, 2018

[6] Y. Bi, T. Zhao, J. Xu, G. Shu, C. Wu and Y. Wang "An Improved Combined Current Control for Single-Phase Operation Mode of Single-/Three-Phase EV Charging System With Voltage Ripple Suppression," in IEEE Transactions on Power Electronics, vol. 38, no. 11, pp. 13635-13649, Nov. 2023

[7] H. Zhao, Y. Shen, W. Ying, S. S. Ghosh, M. R. Ahmed, and T. Long, "A Single- and Three-Phase Grid Compatible Converter for Electric Vehicle On-Board Chargers," in IEEE Transactions on Power Electronics, vol. 35, no. 7, pp. 7545-7562, Jul. 2020